Simple solutions of an opening in elastic-brittle plastic rock mass by total strain and incremental approaches

Kyungho Park[*]

Department of Civil Engineering, A'Sharqiyah University, Oman

Abstract.   This study deals with simple solutions for a spherical or circular opening excavated in elastic-brittle plastic rock mass compatible with a linear Mohr-Coulomb (M-C) or a nonlinear Hoek-Brown (H-B) yield criterion. Based on total strain approach, the closed-form solutions of stresses and displacement are derived simultaneously for circular and spherical openings using original H-B and M-C yield criteria. Two simple numerical procedures are proposed for the solution of generalized H-B and M-C yield criteria. Based on incremental approach, the similarity solution is derived for circular and spherical openings using generalized H-B and M-C yield criteria. The classical Runge-Kutta method is used to integrate the first-order ordinary differential equations. Using three data sets for M-C and H-B models, the results of the radial displacements, the spreading of the plastic radius with decreasing pressure, and the radial and circumferential stresses in the plastic region are compared. Excellent agreement among the solutions is obtained for all cases of spherical and circular openings. The importance of the use of proper initial values in the similarity solution is discussed.

Keywords: rock; opening; total strain approach; incremental approach; similarity solution; elastic-brittle plastic rock; Hoek-Brown yield criterion

1. Introduction

Prediction of the stresses and displacements around a circular or spherical opening in the rock mass at great depth is an important problem in tunneling and underground space development such as the design of tunnels, boreholes and mine shafts (Zhang and Goh 2016, Nawel and Salah 2015, Vrakas and Anagnostou 2014, Wang *et al.* 2012). The analytical and numerical solutions for a spherical or circular opening problem have been developed by considering different models of material behavior, such as the elastic-perfectly plastic, elastic-brittle plastic and elastic-strain softening models, with the different yield criteria, like the linear Mohr-Coulomb (M-C) and nonlinear Hoek-Brown (H-B) criteria (Fahimifar *et al.* 2015, Serrano *et al.* 2011, Shin *et al.* 2011, Osgoui and Oreste 2010, Brown *et al.* 1983).

The analysis for a spherical or circular opening excavated in elastic-brittle plastic rock mass can be carried out using mainly two alternative solution procedures: total strain approach and incremental approach. In total strain approach, the incremental form of the plastic flow rule is integrated directly to result in a relationship between total stresses and total strains. Brown *et al.*

---

[*]Corresponding author, Ph.D., E-mail: khpark.tanzania@gmail.com

(1983) presented closed-form solutions for the stresses and displacements of a circular opening in original H-B medium, followed by Sharan (2003, 2005, 2008) and Park and Kim (2006). Recently, Wang and Yin (2011) presented the closed-form solution of a spherical opening in M-C and original H-B media.

The incremental approach relates stress to plastic strain increments and therefore involves space and time variables; as a result, it requires solving partial differential equations. Similarity solution method, based on incremental approach, has been used to analyze the opening problems (Detournay 1986, Carranza-Torres and Fairhurst 1999, Alonso *et al.* 2003, Park 2014a,b). In the method, partial differential equations are replaced by a small number of first-order ordinary differential equations, which can be solved by using relatively simple computational methods. Carranza-Torres (2004) presented the similarity solution for a circular opening excavated in the elastic-brittle plastic generalized H-B rock mass.

From the literature review, it is noted that the closed-form solution has been developed using original H-B and M-C yield criteria, whereas numerical solutions have been developed for generalized H-B criterion.

The main objective of this study is to examine the solutions, based on both total strain and incremental approaches, for a spherical or circular opening excavated in elastic-brittle plastic rock mass compatible with M-C or H-B yield criterion. Based on the total strain approach, the closed-form solutions of stresses and displacement are derived simultaneously for circular and spherical openings using original H-B and M-C yield criteria. Two simple numerical procedures are proposed for the solution of generalized H-B and M-C criteria. Based on the incremental approach, the similarity solution is derived simultaneously for circular and spherical openings using generalized H-B and M-C yield criteria. The classical Runge-Kutta (R-K) method is used to integrate the first-order ordinary differential equations of stress and displacement as used for the opening problem in Detournay (1986) and Carranza-Torres (2004). The accuracy and practical application of closed-form solution, similarity solution, and two numerical procedures are illustrated by comparing the results for three data sets using M-C and H-B yield criteria.

2. Definition of the problem

Fig. 1 shows a circular or spherical opening being excavated in a continuous, homogeneous, isotropic, initially elastic rock mass subjected to a hydrostatic stress p_o. The opening surface is subjected to an internal pressure p_i. As p_i is gradually reduced, the radial displacement occurs and a plastic region develops around the opening when p_i is less than the initial yield stress. After yielding, the strength of rock suddenly drops and follows the post-yield behavior. The material behavior of elastic-brittle plastic model used in this study is shown in Fig. 2. It is required to solve for the stresses and displacement in the plastic region.

Two most commonly used yield criteria for the rock are considered in this study: the generalized H-B yield criterion,

$$\sigma_1 = \sigma_3 + \sigma_c \left(\frac{m\sigma_3}{\sigma_c} + s \right)^a \tag{1}$$

and the linear M-C yield criterion,

$$\sigma_1 = \alpha\sigma_3 + Y \tag{2}$$

where σ_1 = the major principal stress at failure, σ_3=the minor principal stress at failure, σ_c=the uniaxial compressive strength of the intact rock material, *a*, *m* and *s* = semi-empirical parameters that characterize the rock mass, $\alpha = (1 + \sin\phi)/(1 - \sin\phi)$, $Y = 2c\cos\phi/(1 - \sin\phi)$, *c*=the cohesion of the rock, and ϕ= the friction angle of the rock.

Because of the axial symmetry of the problem, the radial and tangential stresses, σ_r and σ_θ, in the rock mass will be principal stresses, such as $\sigma_1 = \sigma_\theta$ and $\sigma_3 = \sigma_r$. Then Eqs. (1) and (2) can be expressed as

$$\sigma_\theta = \sigma_r + \sigma_{cp}\left(\frac{m_p\sigma_r}{\sigma_{cp}} + s_p\right)^{a_p} \quad \text{for peak strength} \tag{3}$$

$$\sigma_\theta = \sigma_r + \sigma_{cr}\left(\frac{m_r\sigma_r}{\sigma_{cr}} + s_r\right)^{a_r} \quad \text{for postpeak strength} \tag{4}$$

$$\sigma_\theta = \alpha_p\sigma_r + Y_p \quad \text{for peak strength} \tag{5}$$

$$\sigma_\theta = \alpha_r\sigma_r + Y_r \quad \text{for postpeak strength} \tag{6}$$

where subscript *p* indicates the peak value, while subscript *r* indicates the residual value.

The solutions for circular and spherical openings can be developed simultaneously, with the value of the dimensional parameter *k* being 1 for a circular opening and 2 for a spherical opening (Carranza-Torres and Fairhurst 1999).
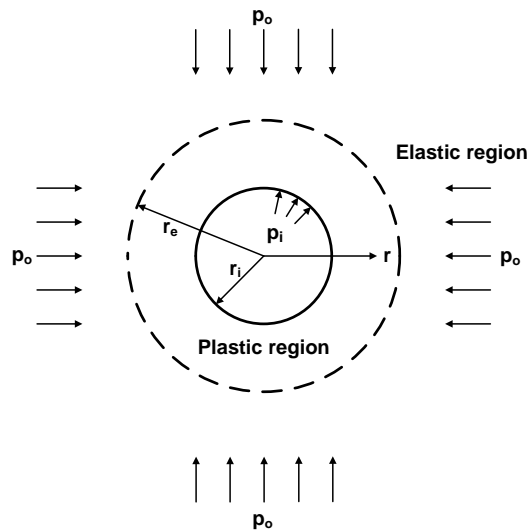

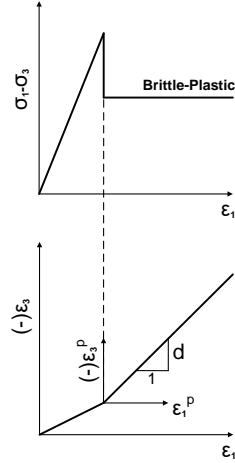Fig. 1 A spherical or circular opening in an infinite medium

Fig. 2 Elastic-brittle plastic model (Brown *et al.* 1983, Park and Kim 2006)

3. Closed-form solution by total strain approach

3.1 Stress equilibrium equation

Assuming a state of plane strain or spherically symmetry around the opening, the equilibrium equation in polar coordinate system is given by

$$\frac{\partial \sigma_r}{\partial r} + \frac{k}{r}(\sigma_r - \sigma_\theta) = 0 \tag{7}$$

where σ_r is the radial stress and σ_θ is the circumferential stress.

3.2 Constitutive equation

The stress-strain relationship, with the consideration of initial hydrostatic stress, for an isotropic elastic material can be written as

$$2G\varepsilon^e = \mathrm{M}(\sigma - p_o) \tag{8}$$

where $\varepsilon^e = \{\varepsilon_r^e, \varepsilon_\theta^e\}^T$ is the vector of elastic strains, $\sigma = \{\sigma_r, \sigma_\theta\}^T$ is the vector of stress components, p_o is the initial stress, G is the shear modulus, superscript e indicates the elastic part, M is a dimensionless compliance matrix, such as

$$\mathrm{M} = \begin{bmatrix} M_{11} & M_{12} \\ M_{21} & M_{22} \end{bmatrix} = \frac{1}{1+(k-1)\nu}\begin{bmatrix} 1-(2-k)\nu & -k\nu \\ -\nu & 1-\nu \end{bmatrix} \tag{9}$$

and ν is the Poisson's ratio.

The plastic strains are expressed in terms of the derivatives of a plastic potential function $g(\sigma_\theta, \sigma_r)$ and given by

$$\varepsilon_r^p = \lambda \frac{\partial g}{\partial \sigma_r} \tag{10}$$

$$k\varepsilon_\theta^p = \lambda \frac{\partial g}{\partial \sigma_\theta} \tag{11}$$

where λ is the plastic multiplier and superscript p indicates the plastic part.

By eliminating the plastic multiplier in Eqs. (10) and (11), the non-associated flow rule can be expressed as

$$d = -\frac{\partial g/\partial \sigma_r}{\partial g/\partial \sigma_\theta} = -\frac{\varepsilon_r^p}{k\varepsilon_\theta^p} \tag{12}$$

where $d = (1 + \sin\psi_r)/(1 - \sin\psi_r)$ and ψ_r is the residual value of dilation angle.

Substituting Eq. (8) into Eq. (12) results in

$$\varepsilon_r + \beta\varepsilon_\theta = \frac{1}{2G}\{A_r(\sigma_r - p_o) + A_\theta(\sigma_\theta - p_o)\} \tag{13}$$

where

$$A_r = M_{11} + \beta M_{21} \; ; \; A_\theta = M_{12} + \beta M_{22} \; ; \; \beta = kd \tag{14}$$

3.3 Closed-form solution

The closed-form solution can be obtained for the original H-B (that is, $a=a_r=0.5$) and M-C yield criteria.

Let's consider the single dimensionless radial coordinate,

$$\rho = \frac{r}{r_e} \tag{15}$$

and the non-dimensionalized forms of radial displacement, u, and stresses

$$\tilde{u} = \frac{2G}{p_1}\frac{u}{r_e} \; ; \; \tilde{\sigma}_r = \frac{\sigma_r}{p_1} \; ; \; \tilde{\sigma}_\theta = \frac{\sigma_\theta}{p_1} \; ; \; \tilde{p}_o = \frac{p_o}{p_1} \tag{16}$$

where r_e is the radius of the plastic region, and p_1 is a suitably chosen reference, such as

$$p_1 = p_o - p_{1y} \tag{17}$$

and p_{1y} is the initial yielding stress.

Then the stress equilibrium equation, Eq. (7) is rewritten as

$$\frac{d\tilde{\sigma}_r}{d\rho} + \frac{k}{\rho}(\tilde{\sigma}_r - \tilde{\sigma}_\theta) = 0 \tag{18}$$

Considering that

$$\varepsilon_r = \frac{p_1}{2G}\frac{d\tilde{u}}{d\rho} \tag{19}$$

$$\varepsilon_\theta = \frac{p_1}{2G}\frac{\tilde{u}}{\rho} \tag{20}$$

the constitutive equation, Eq. (13), is rewritten as

$$\frac{d\tilde{u}}{d\rho} + \beta\frac{\tilde{u}}{\rho} = A_r(\tilde{\sigma}_r - \tilde{p}_o) + A_\theta(\tilde{\sigma}_\theta - \tilde{p}_o) \tag{21}$$

Eqs. (4) and (6) are also rewritten as

$$\tilde{\sigma}_\theta = \tilde{\sigma}_r + \frac{\sigma_{cr}}{p_1}\left(\frac{m_r p_1 \tilde{\sigma}_r}{\sigma_{cr}} + s_r\right)^{a_r} \tag{22}$$

$$\tilde{\sigma}_\theta = \alpha_r\tilde{\sigma}_r + \frac{Y_r}{p_1} \tag{23}$$

3.3.1 Solution for stresses

By substituting Eq. (22) into Eq. (18) and using the boundary condition at the inner face, that is $\tilde{\sigma}_r = \tilde{p}_i$ at $\rho = \rho_i$, the stresses in the plastic region can be obtained for original H-B yield criterion

$$\tilde{\sigma}_r = \tilde{p}_i + A^{H-B}\,\ell n\left(\frac{\rho}{\rho_i}\right) + B^{H-B}\,\ell n^2\left(\frac{\rho}{\rho_i}\right) \tag{24}$$

$$\tilde{\sigma}_\theta = \tilde{p}_i + \frac{A^{H-B}}{k} + \left(A^{H-B} + \frac{2B^{H-B}}{k}\right)\ell n\left(\frac{\rho}{\rho_i}\right) + B^{H-B}\,\ell n^2\left(\frac{\rho}{\rho_i}\right) \tag{25}$$

where

$$A^{H-B} = \frac{k\sigma_{cr}}{p_1}\sqrt{\frac{m_r}{\sigma_{cr}}p_1\tilde{p}_i + s_r}\ ,\quad B^{H-B} = \frac{k^2 m_r \sigma_{cr}}{4p_1} \tag{26}$$

and the superscript *H-B* represents the Hoek-Brown yield criterion.

The most inner radius ρ_i can be obtained by considering the continuity of the radial stress at the elastic-plastic interface.

$$\rho_i = \exp\left\{\frac{A^{H-B} - \sqrt{A^{H-B^2} - 4B^{H-B}(\tilde{p}_i - \tilde{p}_o + 1)}}{2B^{H-B}}\right\} \tag{27}$$

The radius of the plastic region r_e is obtained from Eqs. (15) and (27)

$$r_e = \frac{r_i}{\rho_i} \tag{28}$$

where r_i is the radius of opening.

In the same way, using Eq. (23), the stresses in the plastic region and the radius of the plastic region can be obtained for M-C criterion

$$\tilde{\sigma}_r = A^{M-C} + B^{M-C} \left(\frac{\rho}{\rho_i}\right)^{k(\alpha_r-1)} \tag{29}$$

$$\tilde{\sigma}_\theta = A^{M-C} + B^{M-C} \alpha_r \left(\frac{\rho}{\rho_i}\right)^{k(\alpha_r-1)} \tag{30}$$

$$r_e = \frac{r_i}{\rho_i} = r_i \left\{ \frac{\tilde{p}_o - 1 - A^{M-C}}{B^{M-C}} \right\}^{\frac{1}{k(\alpha_r-1)}} \tag{31}$$

where

$$A^{M-C} = -\frac{Y_r}{p_1(\alpha_r-1)}, \quad B^{M-C} = \tilde{p}_i + \frac{Y_r}{p_1(\alpha_r-1)} \tag{32}$$

and the superscript *M-C* represents the Mohr-Coulomb yield criterion.

3.3.2 Solution for displacement

The integration in Eq. (21) can be made analytically and the solution for the radial displacement can be simplified as

$$\frac{\tilde{u}}{\rho} = \frac{1}{\rho^{\beta+1}} \left\{ D_1 f_1(\rho) + D_2 f_2(\rho) + D_3 f_3(\rho) + \tilde{u}(1) - D_1 f_1(1) - D_2 f_2(1) - D_3 f_3(1) \right\} \tag{33}$$

where

$$f_1(\rho) = \int \rho^\beta d\rho = \frac{\rho^{\beta+1}}{\beta+1} \tag{34}$$

$$f_2^{H-B}(\rho) = \int \rho^\beta \ell n\left(\frac{\rho}{\rho_i}\right) d\rho = \frac{\rho^{\beta+1}}{\beta+1} \left\{ \ell n\left(\frac{\rho}{\rho_i}\right) - \frac{1}{\beta+1} \right\} \tag{35}$$

$$f_2^{M-C}(\rho) = \int \rho^\beta \left(\frac{\rho}{\rho_i}\right)^{k(\alpha_r-1)} d\rho = \frac{1}{\rho_i^{k(\alpha_r-1)}} \frac{\rho^{\beta+k(\alpha_r-1)+1}}{\beta+k(\alpha_r-1)+1} \tag{36}$$

$$f_3^{H-B}(\rho) = \int \rho^\beta \ell n^2\left(\frac{\rho}{\rho_i}\right) d\rho = \frac{\rho^{\beta+1}}{\beta+1} \left\{ \ell n^2\left(\frac{\rho}{\rho_i}\right) - \frac{2}{\beta+1} \ell n\left(\frac{\rho}{\rho_i}\right) + \frac{2}{(\beta+1)^2} \right\} \tag{37}$$

Table 1 Summary of the constants and functions for Eq. (33)

	H-B	M-C
D_1	$\left(A_r + A_\theta\right)\left(\tilde{p}_i - \tilde{p}_o\right) + \dfrac{AA_\theta}{k}$	$A_r\left(A - \tilde{p}_o\right) + A_\theta\left(\alpha_r A + \dfrac{Y_r}{p_1} - \tilde{p}_o\right)$
D_2	$\left(A_r + A_\theta\right)A + \dfrac{2BA_\theta}{k}$	$\left(A_r + \alpha_r A_\theta\right)B$
D_3	$\left(A_r + A_\theta\right)B$	0
$f_1(\rho)$	$\dfrac{\rho^{\beta+1}}{\beta+1}$	
$f_2(\rho)$	$\dfrac{\rho^{\beta+1}}{\beta+1}\left\{\ell n\left(\dfrac{\rho}{\rho_i}\right) - \dfrac{1}{\beta+1}\right\}$	$\dfrac{1}{\rho_i^{k(\alpha_r-1)}}\dfrac{\rho^{\beta+k(\alpha_r-1)+1}}{\beta+k(\alpha_r-1)+1}$
$f_3(\rho)$	$\dfrac{\rho^{\beta+1}}{\beta+1}\left\{\ell n^2\left(\dfrac{\rho}{\rho_i}\right) - \dfrac{2}{\beta+1}\ell n\left(\dfrac{\rho}{\rho_i}\right) + \dfrac{2}{(\beta+1)^2}\right\}$	0
r_e	$r_i \exp\left\{\dfrac{-A + \sqrt{A^2 - 4B\left(\tilde{p}_i - \tilde{p}_o + 1\right)}}{2B}\right\}$	$r_i\left\{\dfrac{\tilde{p}_o - 1 - A}{B}\right\}^{\frac{1}{k(\alpha_r-1)}}$
A	$\dfrac{k\sigma_{cr}}{p_1}\sqrt{\dfrac{m_r}{\sigma_{cr}}p_1\tilde{p}_i + s_r}$	$-\dfrac{Y_r}{p_1\left(\alpha_r - 1\right)}$
B	$\dfrac{k^2 m_r \sigma_{cr}}{4p_1}$	$\tilde{p}_i + \dfrac{Y_r}{p_1\left(\alpha_r - 1\right)}$
p_{1y}	$p_o - \dfrac{\sigma_c}{2}\left(\dfrac{k}{1+k}\right)^2\left\{\sqrt{m_p^2 + 4\left(\dfrac{1+k}{k}\right)^2\left(\dfrac{m_p p_o}{\sigma_c} + s_p\right)} - m_p\right\}$	$\dfrac{\left(1+k\right)p_o - kY_p}{k\alpha_p + 1}$
$\tilde{u}(1)$		$\dfrac{1}{k}$

and $\tilde{u}(1)$, $f_1(1)$, $f_2(1)$, $f_3(1)$ are the values at $\rho=1$.

Table 1 summarizes the constants, D_1, D_2 and D_3, and functions, $f_1(\rho)$, $f_2(\rho)$ and $f_3(\rho)$, for original H-B and M-C yield criteria.

4. Numerical procedures for generalized H-B criterion

It is noted that the necessary equations for the closed-form solutions, Eqs. (18) and (21), obtained from stress equilibrium and constitutive law, are first-order ordinary differential equations.

For the generalized H-B criterion, two numerical procedures can be proposed:

(1) Numerical Procedure-1

In Numerical Procedure-1, Eqs. (18) and (21) are rearranged as

$$\frac{d\tilde{\sigma}_r}{d\rho} = \frac{k\sigma_{cr}}{\rho p_1}\left(\frac{m_r p_1 \tilde{\sigma}_r}{\sigma_{cr}} + s_r\right)^{a_r}$$ (38)

$$\frac{d\tilde{u}}{d\rho} = -\beta\frac{\tilde{u}}{\rho} + A_r\left(\tilde{\sigma}_r - \tilde{p}_o\right) + A_\theta\left(\tilde{\sigma}_\theta - \tilde{p}_o\right)$$ (39)

Here $\tilde{\sigma}_\theta$ is obtained by Eq. (22).

(2) Numerical Procedure-2

In Numerical Procedure-2, instead of Eq. (22), Eq. (40) is used

$$\frac{d\tilde{\sigma}_\theta}{d\rho} = \left\{1 + m_r a_r\left(\frac{m_r p_1 \tilde{\sigma}_r}{\sigma_{cr}} + s_r\right)^{a_r - 1}\right\}\frac{d\tilde{\sigma}_r}{d\rho}$$ (40)

as well as Eqs. (38) and (39).

In order to obtain the solution from Eqs. (38)-(40), the standard ordinary differential equation system solver library routines can be used. In this study, the classical fourth-order R-K method is used without any adaptive step size (Chapra and Canale 2002).

4.1 Initial values at elastic-plastic boundary

Using the solutions for stress and displacement in the outer elastic region given by

$$\sigma_r = p_o + \left(p - p_o\right)\left(\frac{r_e}{r}\right)^{1+k}$$ (41)

$$u = \frac{\left(p_o - p\right)}{2kG}\left(\frac{r_e}{r}\right)^{1+k} r$$ (42)

the necessary initial values at $\rho=1$ can be obtained as

$$\tilde{\sigma}_r(1) = \tilde{p}_o - 1$$ (43)

$$\tilde{u}(1) = \frac{1}{k}$$ (44)

The initial value of $\tilde{\sigma}_\theta$ is obtained from the yield criterion, such as

$$\tilde{\sigma}_\theta(1) = \tilde{\sigma}_r(1) + \frac{\sigma_{cr}}{p_1}\left(\frac{m_r p_1 \tilde{\sigma}_r(1)}{\sigma_{cr}} + s_r\right)^{a_r}$$ (45)

5. Similarity solution by incremental approach

In the previous section, two first-order ordinary differential equations for stress and radial

displacement are used for the analysis. On the other hand, the second-order ordinary differential equation for radial displacement was used in the previous study by Carranza-Torres (2004). In this section, the derivation of the second-order ordinary differential equation for radial displacement is made using the rate forms of stress and strain.

5.1 Constitutive equation

The elastic stress-strain relationship for an isotropic elastic material can be written in the rate form

$$2G\dot{\varepsilon}^e = \mathrm{M}\dot{\sigma} \tag{46}$$

where $\dot{\varepsilon}^e = \left\{\dot{\varepsilon}_r^e, \dot{\varepsilon}_\theta^e\right\}^T$ is the vector of elastic strain rates, $\dot{\sigma} = \left\{\dot{\sigma}_r, \dot{\sigma}_\theta\right\}^T$ is the vector of stress rates. Considering the non-associated flow rule of Eq. (12), Eq. (46) becomes

$$\dot{\varepsilon}_r + \beta\dot{\varepsilon}_\theta = \frac{1}{2G}\left(A_r\dot{\sigma}_r + A_\theta\dot{\sigma}_\theta\right) \tag{47}$$

5.2 Displacement equation

Now let's consider the single dimensionless radial coordinate,

$$\rho = \frac{r}{r_e} = \frac{r}{\tau} \tag{48}$$

and the non-dimensionalized forms of radial displacement and stresses

$$\tilde{u} = \frac{2G}{p_1}\frac{u}{\tau} \quad ; \quad \tilde{\sigma}_r = \frac{\sigma_r}{p_1} \quad ; \quad \tilde{\sigma}_\theta = \frac{\sigma_\theta}{p_1} \tag{49}$$

where τ is the fictitious time variable.

From Eq. (48), the time and space derivatives occurring in the governing partial differential equations can be expressed in terms of the single ordinary derivative $d/d\rho$, such as

$$\frac{\partial}{\partial r} = \frac{1}{r_e}\left(\frac{d}{d\rho}\right) \quad ; \quad (\dot{}) = \frac{\partial}{\partial\tau} = -\frac{\rho}{r_e}\left(\frac{d}{d\rho}\right) \tag{50}$$

Considering that

$$\dot{u} = \frac{p_1}{2G}\left(\tilde{u} - \rho\frac{d\tilde{u}}{d\rho}\right) \tag{51}$$

$$\dot{\varepsilon}_r = \frac{\partial\dot{u}}{\partial r} = -\frac{p_1}{2G}\frac{\rho}{r_e}\frac{d^2\tilde{u}}{d\rho^2} \tag{52}$$

$$\dot{\varepsilon}_\theta = \frac{\dot{u}}{r} = \frac{p_1}{2Gr_e}\left(\frac{\tilde{u}}{\rho} - \frac{d\tilde{u}}{d\rho}\right)$$

(53)

the constitutive equation, Eq. (47), is rewritten as

$$\frac{d^2\tilde{u}}{d\rho^2} + \frac{\beta}{\rho}\frac{d\tilde{u}}{d\rho} - \frac{\beta}{\rho^2}\tilde{u} = A_r\frac{d\tilde{\sigma}_r}{d\rho} + A_\theta\frac{d\tilde{\sigma}_\theta}{d\rho}$$

(54)

It is noted that Eq. (54) is the second-order ordinary differential equation, which is similar type used by Carranza-Torres (2004). Eq. (54) can also be obtained directly by taking a derivative of Eq. (21) with respect to ρ.

5.3 Numerical implementation

In order to obtain the similarity solution, four equations are needed: Eq. (38) for $d\tilde{\sigma}_r/d\rho$, Eq. (40) for $d\tilde{\sigma}_\theta/d\rho$, and

$$\frac{d\tilde{\upsilon}}{d\rho} = -\frac{\beta}{\rho}\tilde{\upsilon} + \frac{\beta}{\rho^2}\tilde{u} + A_r\frac{d\tilde{\sigma}_r}{d\rho} + A_\theta\frac{d\tilde{\sigma}_\theta}{d\rho}$$

(55)

$$\frac{d\tilde{u}}{d\rho} = \tilde{\upsilon}$$

(56)

For the solutions of Eqs. (38), (40), (55) and (56), the R-K method is again used without any adaptive step size.

5.4 Initial values at the elastic-plastic boundary

For an elastic-strain softening model, Alonso *et al.* (2003) derived the initial values at $\rho=1$ using the solutions for stress and displacement in the outer elastic region, such as

$$\tilde{\sigma}_\theta(1) = \tilde{p}_o + \frac{1}{k}$$

(57)

$$\tilde{\upsilon}(1) = -1$$

(58)

as well as Eqs. (43) and (44). In the elastic-brittle plastic model, however $\tilde{\sigma}_\theta(1)$ and $\tilde{\upsilon}(1)$ in the plastic region is suddenly changed from those in the elastic region. So the initial values of Eqs. (57) and (58) cannot be used in the analysis of elastic-brittle plastic model. Even in the analysis of elastic-strain softening model, if the model is suddenly changed from elastic to residual regions through the softening region, the use of Eqs. (57) and (58) can cause the unstable results.

In this study, instead of using Eqs. (57) and (58), the initial value of $\tilde{\sigma}_\theta$ is obtained from the yield criterion, such as Eq. (45), and the initial value of $\tilde{\upsilon}$ is obtained from Eq. (21), such as

$$\tilde{\upsilon}(1) = \frac{d\tilde{u}}{d\rho}(1) = -\beta\frac{\tilde{u}(1)}{\rho} + A_r\left(\tilde{\sigma}_r(1) - \tilde{p}_o\right) + A_\theta\left(\tilde{\sigma}_\theta(1) - \tilde{p}_o\right)$$

(59)

It is noted that Carranza-Torres (2004) also used the similar equation for initial value of $\tilde{\upsilon}$.

6. Application

In order to show the applicability and accuracy of the proposed solutions, the results of the radial displacements, the variations of r_e/r_i (which can show the spreading of the plastic radius with decreasing pressure), and the radial and circumferential stresses in the plastic region are compared using three data sets.

Tables 2 and 3 show the data set for original H-B and M-C criteria, respectively. These data sets are used to compare the results among closed-form solution, similarity solution, and two numerical procedures. Table 4 shows the Data Set 3, which is used to show the application of numerical procedures and similarity solution for the generalized H-B criterion.

Figs. 3-5 show the results of the radial displacements at the opening surface and the variations of r_e/r_i, and the radial and circumferential stresses within the plastic region for each data set. Since the solutions for circular and spherical openings have been developed simultaneously, the results are shown together, using $k=1$ for a circular opening and $k=2$ for a spherical opening in the figures.

Table 2 Data Set 1 (original H-B criterion)

Radius of opening, r_i	5.35 m	Initial stress, p_o	3.31 MPa
Young's Modulus, E	1380 MPa	Poisson's ratio, v	0.25
σ_c	27.6 MPa	a	0.5
m_p	0.5	m_r	0.1
s_p	0.001	s_r	0
ψ_p	19.47°	ψ_r	5.22°

Table 3 Data Set 2 (M-C criterion)

Radius of opening, r_i	3.0 m	Initial stress, p_o	20 MPa
Young's modulus, E	10 GPa	Poisson's ratio, v	0.25
c_p	1.0 MPa	c_r	0.7 MPa
ϕ_p	30°	ϕ_r	22°
$\psi_p = \psi_r$	3.75°		

Table 4 Data Set 3 (Carranza-Torres 2004)

Radius of opening, r_i	2 m	Initial stress, p_o	15 MPa
Young's Modulus, E	5.7 MPa	Poisson's ratio, v	0.3
σ_{cp}	30 MPa	σ_{cr}	25 MPa
a_p	0.55	a_r	0.6
m_p	1.7	m_r	0.85
s_p	0.0039	s_r	0.0019
$\psi_p = \psi_r$	0		

(a) Ground response curve

(b) Variation of r_e/r_i

(c) Variation of radial stress for $p_i=0$

(d) Variation of circumferential stress for $p_i=0$
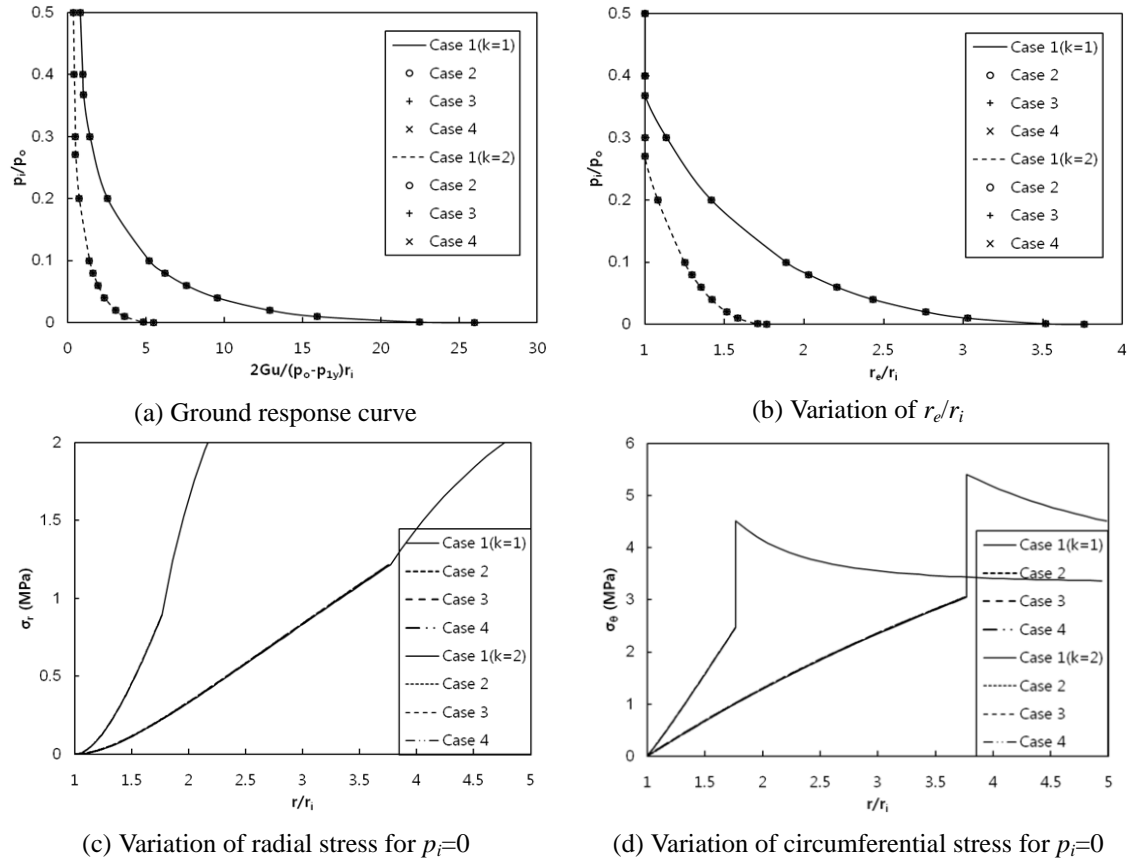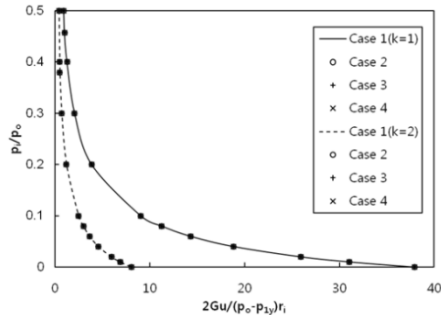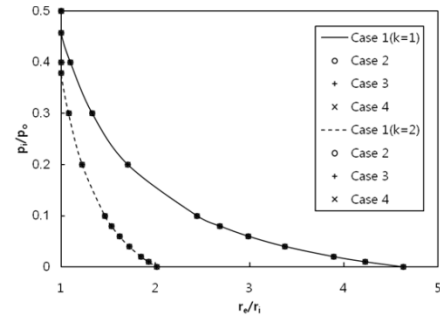
Fig. 3 Results for Data Set 1

Table 5 Results of radial displacements ($2Gu/(p_o-p_{1y})r_i$) at the opening surface

|	(a) Circular opening					(b) Spherical opening			
p_i/p_o	Case 1	Case 2	Case 3	Case 4	p_i/p_o	Case 1	Case 2	Case 3	Case 4
0.5	0.7903	0.7903	0.7903	0.7903	0.5	0.3427	0.3427	0.3427	0.3427
0.4	0.9484	0.9484	0.9484	0.9484	0.4	0.4112	0.4112	0.4112	0.4112
0.3673	1.0	1.0	1.0	1.0	0.3	0.4798	0.4798	0.4798	0.4798
0.3	1.4155	1.4154	1.4154	1.4154	0.2705	0.5	0.5	0.5	0.5
0.2	2.5323	2.5323	2.5323	2.5323	0.2	0.7286	0.7286	0.7286	0.7286
0.1	5.2041	5.2041	5.2041	5.2041	0.1	1.3861	1.3861	1.3861	1.3861
0.08	6.2156	6.2156	6.2156	6.2156	0.08	1.6204	1.6204	1.6204	1.6204
0.06	7.5854	7.5855	7.5855	7.5855	0.06	1.9280	1.9280	1.9280	1.9280
0.04	9.5785	9.5786	9.5786	9.5786	0.04	2.3586	2.3586	2.3586	2.3586
0.02	12.9288	12.9289	12.9288	12.9288	0.02	3.0471	3.0472	3.0472	3.0472
0.01	15.9455	15.9456	15.9456	15.9456	0.01	3.6377	3.6377	3.6377	3.3677
0.001	22.4643	22.4649	22.4649	22.4649	0.001	4.8433	4.8434	4.8434	4.8434

(a) Ground response curve
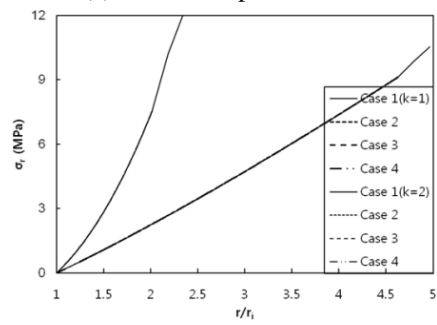
(b) Variation of r_e/r_i

(c) Variation of radial stress for $p_i=0$
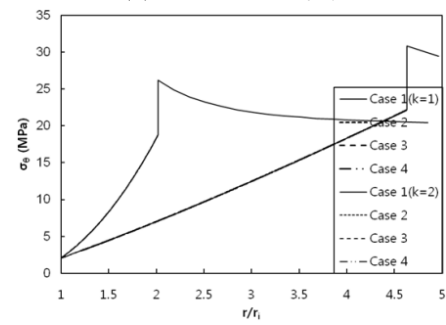
(d) Variation of circumferential stress for $p_i=0$

Fig. 4 Results for Data Set 2
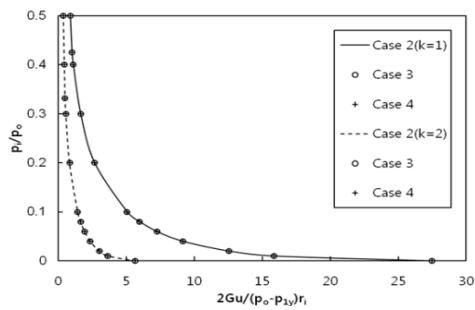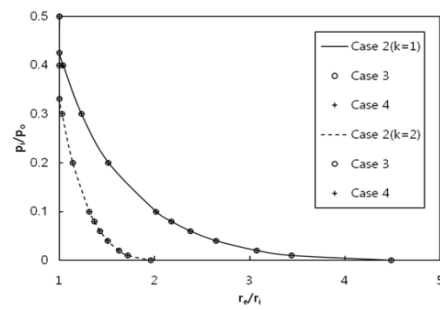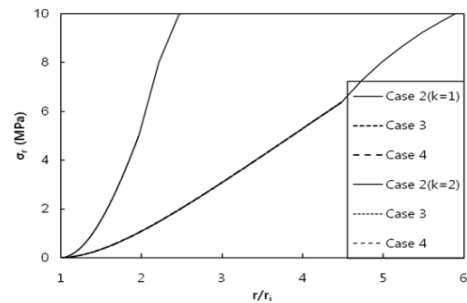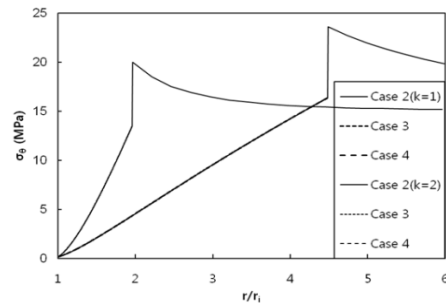

(a) Ground response curve

(b) Variation of r_e/r_i

(c) Variation of radial stress for $p_i=0$

(d) Variation of circumferential stress for $p_i=0$

Fig. 5 Results for Data Set 3

Case-1, 2, 3, and 4 indicate the results by closed-form solution (using Eqs. (29), (30) and (33)), Numerical Procedure-1 (Eqs. (38), (22) and (39)), Numerical Procedure-2 (Eqs. (38), (40) and (39)), and similarity solution (Eqs. (38), (40), (55) and (56)), respectively. The step size of h=0.0001 is used for numerical procedures and similarity solution.

For the quantitative comparison, the results of the radial displacement at the surface opening, as shown in Fig. 3(a), are summarized for circular and spherical openings in Table 5.

From Figs. 3-5 and Table 5, the following observations can be made:

(1) Excellent agreement among the results from closed-form solution, similarity solution, and numerical procedures can be seen for Data Set 1 and Set 2 in both circular and spherical openings. Thus, the accuracy of the proposed numerical procedures and similarity is satisfactory. It is noted that the results by the presented closed-form solution are also compared with those by the previous closed-form solution of Park and Kim (2006). The identical results are obtained from two solutions.

(2) Excellent agreement among the results from similarity solution and two numerical procedures can be seen for Data Set 3 in both circular and spherical openings. Thus, the applicability of the proposed solutions in the analysis of generalized H-B and M-C yield criteria is further verified.

(3) The displacements induced by opening from the spherical solution are about 4.7-4.9 times smaller than those from the circular solution. As expected, the range of plastic region induced by opening from the spherical solution is about 2.1-2.3 smaller than those from the circular solution.

(4) The use of initial values, such as Eq. (45) for $\tilde{\sigma}_{\theta}$ and Eq. (59) for $\tilde{\upsilon}$, is verified. Those initial values and similarity solution can be used for the analysis of elastic-strain softening model (Park 2014a).

7. Conclusions

Simple analytical and numerical solutions of the stresses and displacement for a spherical or circular opening excavated in elastic-brittle plastic rock masses compatible with M-C and H-B yield criteria have derived based on both total strain and incremental approaches. The accuracy and practical application of the proposed solutions were illustrated by solving three examples.

Excellent agreement among the results from closed-form solution, similarity solution, and numerical procedures were obtained in both circular and spherical openings using the data set of H-B and M-C yield criteria. The importance of the use of proper initial values in the similarity solution is discussed.

Although the solutions proposed in this paper are limited in scope, it appears to be useful for the preliminary design of a spherical or circular rock opening to obtain the ground response curve. The solutions can also be used for the validation of numerical methods, such as the finite element method.

References

Alonso, E., Alejano, L.R., Varas, F., Fdez-Manin, G. and Carranza-Torres, C. (2003), "Ground response curves for rock masses exhibiting strain-softening behavior", *I. J. Numer. Anal. Meth. Geomech.*, **27**(13), 1153-1185.

Brown, E.T., Bray, J.W., Ladanyi, B. and Hoek, E. (1983), "Ground response curves for rock tunnels", *J. Geotech. Eng.*, **109**(1), 15-39.

Carranza-Torres, C. (2004), "Elasto-plastic solution of tunnel problems using the generalized form of the Hoek-Brown failure criterion", *I. J. Rock Mech. Min. Sci.*, **41**(3), 480-481.

Carranza-Torres, C. and Fairhurst, C. (1999), "The elasto-plastic response of underground excavations in rock masses that satisfy the Hoek-Brown failure criterion", *I. J. Rock Mech. Min. Sci.*, **36**(5), 777-809.

Chapra, S.C. and Canale, R.P. (2002), *Numerical Methods for Engineers*, 4th Edition, McGraw-Hill, New York, U.S.A.

Detournay, E. (1986), "Elastoplastic model of a deep tunnel for a rock with variable dilatancy", *Rock Mech. Rock Eng.*, **19**(2), 99-108.

Fahimifar, A., Ghadami, H. and Ahmadvand, M. (2015), "The ground response curve of underwater tunnels excavated in a strain-softening rock mass", *Geomech. Eng., J.*, **8**(3), 323-359.

Nawel, B. and Salah, M. (2015), "Numerical modeling of two parallel tunnels interaction using three-dimensional finite elements method", *Geomech. Eng.*, **9**(6), 775-791.

Osgoui, R. and Oreste, P. (2010), "Elasto-plastic analytical model for the design of grouted bolts in a hoek-brown medium", *I. J. Numer. Anal. Met. Geomech.*, **34**(16), 1651-1686.

Park, K.H. (2014a), "Similarity solution of a spherical or circular opening in elastic-strain softening rock mass", *I. J. Rock Mech. Min. Sci.*, **71**, 151-159.

Park, K.H. (2014b), "Large strain similarity solution for a spherical or circular opening excavated in elastic-perfectly plastic media", *I. J. Numer. Anal. Met. Geomech.*, **39**(7), 724-737.

Park, K.H. and Kim, Y.J. (2006), "Analytical solution for a circular opening in an elastic-brittle-plastic rock", *I. J. Rock Mech. Min. Sci.*, **43**(4), 616-622.

Serrano, A., Olalla, C. and Reig, I. (2011), "Convergence of circular tunnels in elastoplastic rock masses with non-linear failure criteria and non-associated flow laws", *I. J. Rock Mech. Min. Sci.*, **48**(6), 878-887.

Sharan, S.K. (2003), "Elastic-brittle-plastic analysis of circular openings in Hoek-Brown media", *I. J. Rock Mech. Min. Sci.*, **40**(6), 817-824.

Sharan, S.K. (2005), "Exact and approximate solutions for displacements around circular openings in elastic-brittle-plastic hoek-brown rock", *I. J. Rock Mech. Min. Sci.*, **42**(4), 542-549.

Sharan, S.K. (2008), "Analytical solutions for stresses and displacements around a circular opening in a generalized hoek-brown rock", *I. J. Rock Mech. Min. Sci.*, **45**(1), 78-85.

Shin, Y.J., Song, K.I, Lee, I.M. and Cho, G.C. (2011), "Interaction between tunnel supports and ground convergence consideration of seepage forces", *I. J. Rock Mech. Min. Sci.*, **48**(3), 394-405.

Vrakas, A. and Anagnostou, G. (2014), "A finite strain closed-form solution for the elastoplastic ground response curve in tunneling", *I. J. Numer. Anal. Met. Geomech.*, **38**(11), 1131-1148.

Wang, S.L. and Yin, S.D. (2011), "A closed-form solution for a spherical cavity in the elastic-brittle-plastic medium", *Tunn. Underg. Sp. Tech.*, **26**(1), 236-241.

Wang, S.L., Yin, S.D. and Wu, Z.J. (2012), "Strain-softening analysis of a spherical cavity", *I. J. Numer. Anal. Met. Geomech.*, **36**(2), 182-202.

Zhang, W. and Goh, A.T.C. (2016), "Predictive models of ultimate and serviceability performances for underground twin caverns", *Geomech. Eng.*, **10**(2), 175-188.

CC